Investigation of the Flame Kernel Propagation after Ignition by a Low Energy Electrical Discharge

Stefan Essmann[a], Detlev Markus[a], and Ulrich Maas[b]
[a]Physikalisch-Technische Bundesanstalt, Bundesallee 100, Braunschweig, Germany
[b]Karlsruhe Institute of Technology, Institute of Technical Thermodynamics, Karlsruhe, Germany

1 Introduction

In safety engineering and process industry, electrostatic discharges frequently pose a risk as ignition sources for burnable gas/air mixtures. The forced ignition inside spark engines has been examined in detail both experimentally and numerically (see e.g. [1–3]). However, there is a lack of knowledge concerning the physical and chemical processes during the ignition by electrical discharges relevant in process safety. In order to estimate the risk and to mitigate explosion hazards due to such discharges, safety characteristic data such as the minimum ignition energy (MIE) of the burnable gases are regularly used. The MIE does not only depend on the substance under investigation but also on the test method, specifically the electrode geometry and discharge characteristics. When the ignition energy is close to the MIE, loss processes play an important role, i.e. portions of the electrical input energy that do not contribute to the ignition. They include external (ohmic) losses, heat transfer to the electrodes, radiation, and losses due to the generation of a shock wave [4]. In this energy region, ignition is a stochastic process in practice so that there is only a limited probability of ignition. For instance, the ignition probability at the MIE is around 0.1 % to 1 % [5–7]. Bane et al. have investigated the statistical nature of spark ignition and the role of the MIE in great detail for a range of combustibles [8–10].

In this study, we investigate the ignition by electrical discharges near the MIE experimentally. First, high speed schlieren videos of the early flame propagation following the discharge are recorded for three burnable gas/air mixtures and several energy levels. The effects of discharge energy on the propagation speed and the reproducibility are discussed. Second, optical emission spectroscopy (OES) is employed to the discharges. The vibrational and rotational temperatures are determined from the comparison of experimental spectra with numerical ones.

Correspondence to: stefan.essmann@ptb.de

2 Early Flame Kernel Propagation

2.1 Experiment

The electrical discharges were generated between rounded tungsten rod electrodes placed in a stainless steel vessel at atmospheric pressure (1 bar $\pm$ 40 mbar) and room temperature (21.5 $\pm$ 1.0 °C). They were triggered by the frequency quadrupled radiation from an Nd:YAG laser at 266 nm. The most ignitable hydrogen/air, ethylene/air, and propane/air mixtures were ignited by discharges with energies close to the respective MIE (table 1) at ambient, quiescent conditions. The discharge energy was calculated as $E_s = 1/2\ C\,U^2$, where C is the capacitance of the setup and U is the voltage at breakdown. A typical discharge had a duration of 50 ns. For each configuration, the experiment was carried out at least five times. A two-lens schlieren setup with an inverse pinhole used as the schlieren stop was set up in order to visualize the flame. A high-power LED (Luminus SBT-70-G) in continuous wave mode provided sufficient light for imaging the signal on a high speed camera (Photron Fastcam SA-5) at 62 500 frames/s. A Matlab script was used to postprocess the images and determine the position of the flame for each frame. More details concerning the experimental setup can be found in [12].

Table 1: Burnable gas/air mixtures, respective MIE energies [11], and electrode distances (as determined in [6]).

Gas	Conc.	MIE	Electrode distance
Hydrogen	23.3 %	17 µJ	0.5 mm
Ethylene	8.0 %	82 µJ	1.2 mm
Propane	5.2 %	240 µJ	1.7 mm

2.2 Results and Discussion

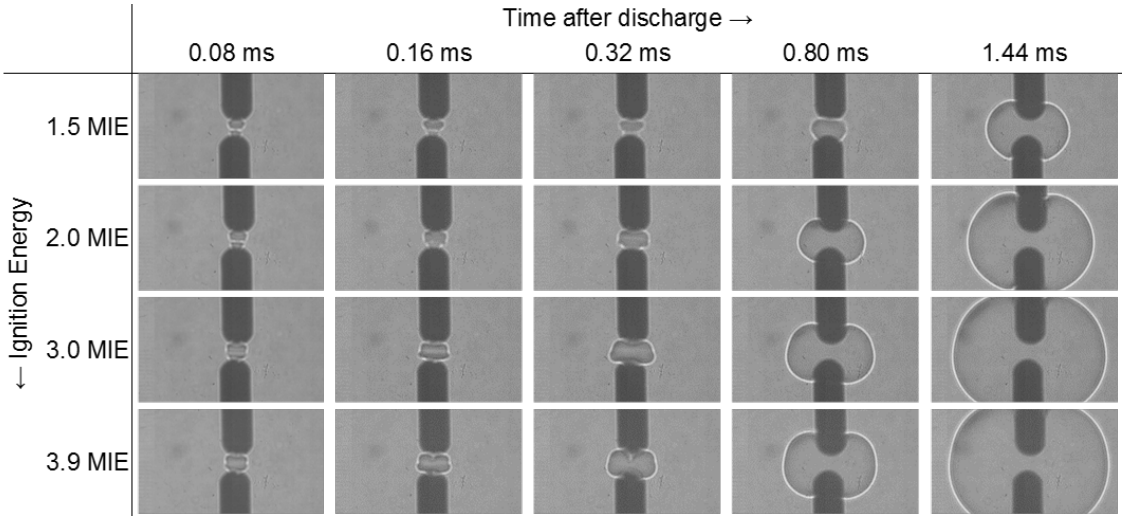

Figure 1: Series of schlieren images showing the early phase of flame kernel expansion in an 8.0 % ethylene/air mixture after ignition by an electrical spark. Each row corresponds to a specific ignition energy indicated on the left while the columns are labeled with the time after ignition. The images were enhanced in brightness and contrast for better visualization.

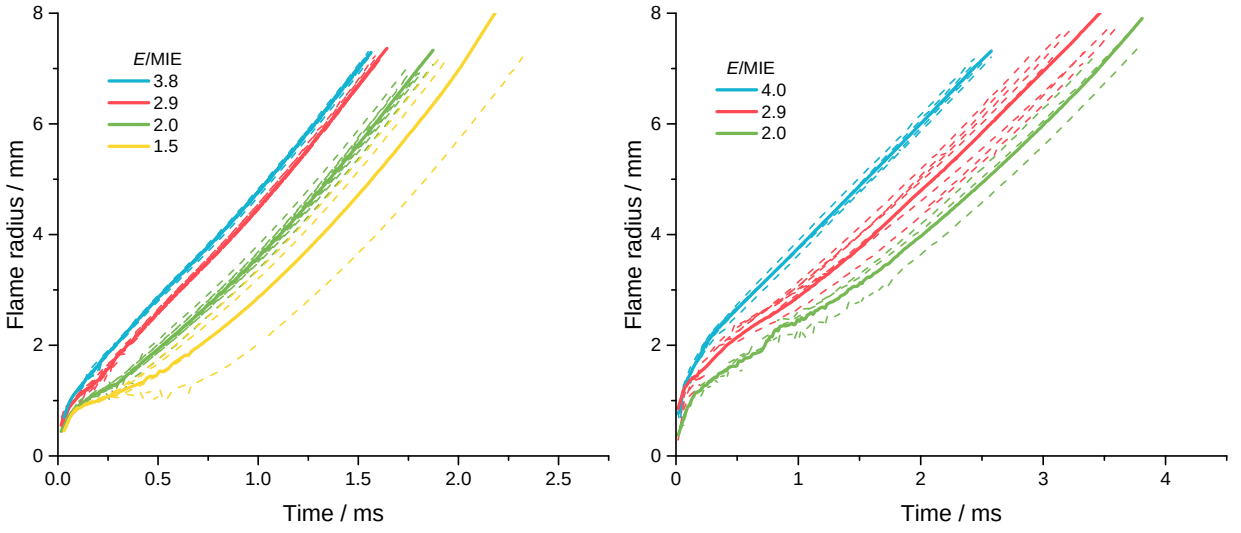

(a) Ethylene (b) Propane

Figure 2: Flame radius as a function of time after discharge for several ignition energies close to the minimum ignition energy. The dashed lines indicate individual experiments; solid, bold lines indicate the respective average values.

Figure 1 shows four series of schlieren images for the ethylene case with ignition energies ranging from 1.5 to about four times the MIE. We can observe that the ignition delay time becomes shorter and that the early flame kernel growth is faster when the ignition energy is increased. The shape of the flame kernel in the first two images of each series (0.08 ms and 0.16 ms) is asymmetric at low energies and becomes more uniform at larger energies. When the ignition energy is sufficiently high, large changes are required for a noticeable change in the early flame kernel propagation while at low energies, the ignition process is very sensitive.

This can also be seen in fig. 2a where the flame front position is plotted against time for ethylene. Only successful ignition events are shown here. At 1.5 and 2.0 MIE, there is considerable scatter between individual experiments which is significantly reduced for the larger energies investigated. Moreover, all curves approach the same slope after about 1 ms. Here, only chemistry and stretch due to the spherical flame shape govern the flame propagation. However, during the first 0.5 ms, the ignition process still plays an important role. The flame kernels of low ignition energy accelerate until the flame speed reaches a constant value. At larger ignition energies, the flames start with a velocity that is even higher, approaching the same flame speed from above. Qualitatively, the same observations are made for the propane (fig. 2b) and hydrogen cases (not shown here). Due to the low Lewis number of the lean hydrogen mixture, the flame propagation is enhanced by curvature at the early stages while for the propane mixture, the Lewis number is significantly larger than unity; hence, the early flame propagation is negatively affected and it takes a longer time for the flame to reach a constant propagation speed [13].

The results show how the ignition process becomes much more reliable and reproducible when the ignition energy is increased. The excess of energy in the discharge volume leads to less sensitivity towards small changes in other parameters concerning the ignition, such as initial temperature and pressure, gas composition, and motion of the gas. Bradley and Lung [14] called this the *spark assisted flame propagation regime* which can last up to several ms, depending on the gas mixture and the ignition energy. The actual physi-

cochemical effects acting inside the discharge region when the energy is increased cannot be inferred from these results though. Qualitatively it is clear that the temperature and pressure become larger. Also, the production of radicals facilitating the ignition process as well as their consumption by wall-interaction may be of importance. In order to gain deeper insight, OES measurements of the discharge were carried out.

3 Optical Emission Spectroscopy of the Discharges

3.1 Experiment

The electrical setup for generating the discharges remained unchanged. Instead of the schlieren setup, an image-intensified detection system was implemented. It consisted of a UV lens (UV-Nikkor 105 mm f/4.5), a spectrograph (Acton Research SpectraPro 300-i) with a 1200 grooves/mm grating installed, an image intensifier (LaVision IRO) and a CCD camera (LaVision Imager ProPlus 2M). The spectral resolution of the system was 0.25 nm. The exposure time of the image intensifier was set to the minimum of 10 ns and the jitter between the laser-triggered discharge and the exposure was ± 10 ns. A mercury-vapor lamp (Newport model 6035) and a halogen lamp (CMS Schreder KS-J1011) were used for spectral and relative intensity calibration, respectively. Electrical discharges were generated in dried air for several electrode distances and discharge energies at 2 Hz repetition rate. Spectrally unresolved images of the discharges were recorded to characterize their temporal and spatial evolution. The spectra of several discharges at identical conditions were recorded on-chip to increase the signal-to-noise ratio. In accordance with [15], the second positive system (SPS) of nitrogen N_2 $\left(C^3\Pi_u, v'\right) \rightarrow \left(B^3\Pi_g, v''\right)$ at 360 nm to 410 nm was compared to a database of numerically simulated spectra (software *Specair*). From the best fit, the rotational and vibrational plasma temperatures T_{rot} and T_{vib} were determined. Since rotational relaxation is fast at atmospheric pressure, the rotational temperature is a good estimate for the translational (gas) temperature [16].

3.2 Results and Discussion

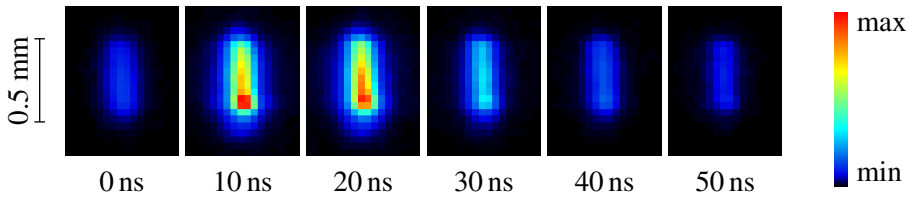

Figure 3: Temporal evolution of the discharge emission (111 µJ discharge energy, 0.5 mm electrode distance). The exposure time of each image was 10 ns.

Figure 3 shows the light emission from a typical discharge at different times during the discharge. The peak intensity is reached after 20 ns. Here, one can observe spatially non-uniform emission where the emission is more intense in a region close to the bottom (grounded) electrode. Spectral analysis showed that while in the rest of the discharge, the SPS of nitrogen is clearly visible, the emission from this area is contains a strong broadband component that partially conceals the features of interest. Therefore, only the region above this broadband spot will be evaluated regarding the temperature. Figure 4 shows typical spectra obtained in this region taken 20 ns after the beginning of the discharge. The electrode distance is constant at 0.5 mm while the energy was changed from 31 to 111 µJ. Even though the energy changes by more than

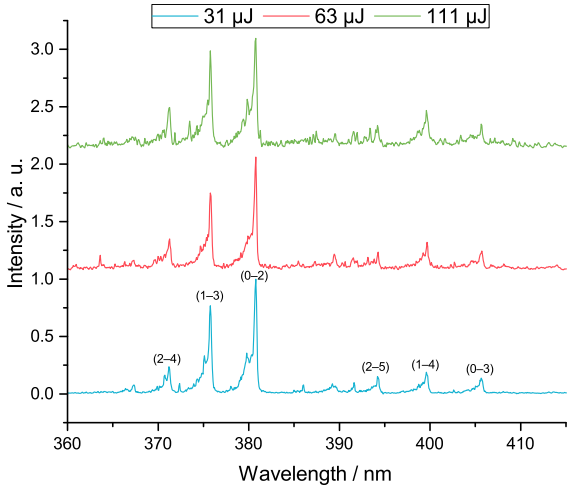

Figure 4: Experimentally obtained spectra at 0.5 mm electrode distance. The most prominent bands in the SPS of nitrogen are indicated.

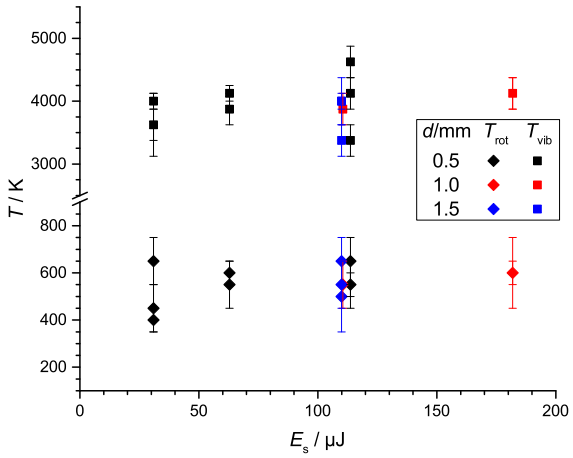

Figure 5: Rotational and vibrational temperatures of the discharges for various electrode distances and discharge energies.

300 %, there are only slight differences in the relative peak intensities of the resulting spectra. In addition, more noise at greater discharge energies limits the precision of the temperature determination. Therefore, no significant differences in the temperatures could be found. Figure 5 shows the rotational and vibrational temperatures found for a range of electrode distances and discharge energies. Duplicate data points refer to measurements of an identical discharge at a different time during the discharge. Due to the limited accuracy of the data, no temporal trend could be found. The rotational and vibrational temperature assigned from the best fit to numerically simulated spectra are in the range 525 ± 125 K and 4000 ± 625 K, respectively, for all electrode distances from 0.5 mm to 1.5 mm and energies from 110 µJ to 180 µJ. These results agree well with findings by Ono et al. [17] who measured T_{rot} to be 430 K to 500 K and T_{vib} to be around 5000 K for discharge energies from 30 µJ to 600 µJ.

4 Conclusion

The ignition process by low energy electrical discharges was investigated experimentally through schlieren measurements of the early flame kernel growth. It was found that close to the MIE, the ignition process exerts a stochastic nature, resulting in poorly reproducible ignition delay times. As the energy is increased, less scatter between repeatedly performed experiments is observed. When the energy is increased to more than 3 to 4 times the MIE, depending on the combustible, the spark assisted flame propagation regime is entered for 0.25 to 0.5 ms where the initial flame propagation speed is elevated due to the ignition source. Some ms after ignition, the flame speed becomes independent of the ignition energy.

Further, the electrical discharges were investigated via OES regarding their rotational and vibrational temperature. However, no statistically significant trend could be resolved by these measurements. Consistent with the work by Ono et al. [17], we found that the discharges are not in local thermodynamic equilibrium and that the temperatures are $T_{\mathrm{rot}} \approx 500$ K and $T_{\mathrm{vib}} \approx 4000$ K, independent of discharge energy or electrode distance (energy density). Temporally resolved images of the discharge emission showed spatial non-uniformity, i.e. greater emission intensities near the grounded electrode.

In future work we plan to perform numerical simulations of the ignition process at energies close to the MIE. The flame kernel data and the temperatures can be directly compared between simulation and experiment. The simulations will provide deeper insight into the physical and chemical processes governing the ignition.

Acknowledgments

Financial support by the Deutsche Forschungsgemeinschaft (DFG) as part of the research group FOR 1447 is gratefully acknowledged.

References

[1] R. R. Maly, "State of the art and future needs in S.I. engine combustion," *Symposium (International) on Combustion*, vol. 25, no. 1, pp. 111–124, 1994.

[2] A. Dreizler, S. Lindenmaier, U. Maas, J. Hult, M. Aldén, and C. F. Kaminski, "Characterisation of a spark ignition system by planar laser-induced fluorescence of OH at high repetition rates and comparison with chemical kinetic calculations," *Applied Physics B: Lasers and Optics*, vol. 70, no. 2, pp. 287–294, 2000.

[3] M. Thiele, J. Warnatz, and U. Maas, "Geometrical study of spark ignition in two dimensions," *Combustion Theory and Modelling*, vol. 4, no. 4, pp. 413–434, 2000.

[4] R. K. Eckhoff and W. Olsen, "A new method for generation of synchronized capacitive sparks of low energy. Reconsideration of previously published findings," *Journal of Electrostatics*, vol. 68, no. 1, pp. 73–78, 2010.

[5] R. K. Eckhoff, M. Ngo, and W. Olsen, "On the minimum ignition energy (MIE) for propane/air," *Journal of Hazardous Materials*, vol. 175, no. 1-3, pp. 293–297, 2010.

[6] A. Wähner, G. Gramse, T. Langer, and M. Beyer, "Determination of the Minimum Ignition Energy on the Basis of a Statistical Approach," in *9th International Symposium on Hazard, Prevention and Mitigation of Industrial Explosions*, 2010.

[7] S. Essmann, D. Markus, and U. Maas, "Investigation of Ignition by Low Energy Capacitance Sparks: Paper P3-45," in *Proceedings of the European Combustion Meeting*, 2013.

[8] S. P. M. Bane, J. L. Ziegler, P. A. Boettcher, S. A. Coronel, and J. E. Shepherd, "Experimental investigation of spark ignition energy in kerosene, hexane, and hydrogen," *Journal of Loss Prevention in the Process Industries*, vol. 26, no. 2, pp. 290–294, 2011.

[9] S. P. M. Bane, J. E. Shepherd, E. Kwon, and A. C. Day, "Statistical analysis of electrostatic spark ignition of lean H2/O2/Ar mixtures," *International Journal of Hydrogen Energy*, vol. 36, no. 3, pp. 2344–2350, 2011.

[10] S. P. M. Bane, "Spark Ignition: Experimental and Numerical Investigation With Application to Aviation Safety," PhD Thesis, California Insitute of Technology, Pasadena, 2010.

[11] E. Brandes and W. Möller, *Flammable liquids and gases: Brennbare Flüssigkeiten und Gase*, 2nd ed., ser. Safety characteristic data. Bremerhaven: Wirtschaftsverl. NW, 2008, vol. 1.

[12] S. Essmann, D. Markus, and U. Maas, "Investigation of the spark channel of electrical discharges near the minimum ignition energy," *Plasma Physics and Technology*, vol. 3, no. 3, pp. 116–121, 2016.

[13] S. C. Taylor, "Burning velocity and the influence of flame stretch," PhD thesis, University of Leeds, Leeds, 1991.

[14] D. Bradley and F. K.-K. Lung, "Spark ignition and the early stages of turbulent flame propagation," *Combustion and Flame*, vol. 69, no. 1, pp. 71–93, 1987.

[15] D. L. Rusterholtz, D. A. Lacoste, G. D. Stancu, D. Z. Pai, and C. O. Laux, "Ultrafast heating and oxygen dissociation in atmospheric pressure air by nanosecond repetitively pulsed discharges," *Journal of Physics D: Applied Physics*, vol. 46, no. 46, p. 464010, 2013.

[16] C. O. Laux, T. G. Spence, C. H. Kruger, and R. N. Zare, "Optical diagnostics of atmospheric pressure air plasmas," *Plasma Sources Science and Technology*, vol. 12, no. 2, pp. 125–138, 2003.

[17] R. Ono, M. Nifuku, S. Fujiwara, S. Horiguchi, and T. Oda, "Gas temperature of capacitance spark discharge in air," *Journal of Applied Physics*, vol. 97, no. 12, p. 123307, 2005.